

## Bad data analysis and detection using PMU with UPQC integration to grid during fault conditions

Preeti Kabra<sup>1</sup>, Suraparaju Venkata Naga Lakshmi Lalitha<sup>1</sup>, Sudha Rani Donepudi<sup>2</sup>

<sup>1</sup>Department of Electrical Engineering, Koneru Lakshmaiah Education Foundation, Vijaywada, India

<sup>2</sup>Department of Electrical Engineering, Sri Vasavi College of Engineering, Tadepalligudem, India

### Article Info

#### Article history:

Received Aug 10, 2022

Revised Nov 13, 2022

Accepted Nov 30, 2022

#### Keywords:

Bad data detection

MATLAB

Phasor measuring units

Principal component analysis

Unified power quality

conditioner

### ABSTRACT

Analysis of bad data in an IEEE 14 bus system with phasor measuring units (PMU) devices is carried out in this paper. The normal operating condition data achieved from the PMU in the bus system is compared to the data achieved during faults in the bus system. A principal component analysis (PCA) technique is proposed in this paper for distinguishing the difference between data transmission during normal and fault conditions. The PCA approach detects the dynamical magnitudes of the measurements taken and also determines the noise caused by the disturbances. The grid system is updated with unified power quality conditioner (UPQC) improving the parameters of the system to mitigate the fault. The PMU devices use PCA technique for a comparative analysis of the measured components analyzing the performance of the system under different operating conditions. The simulation of these modules is carried out in Simulink environment of MATLAB software with PCA done concerning time.

*This is an open access article under the [CC BY-SA](https://creativecommons.org/licenses/by-sa/4.0/) license.*



### Corresponding Author:

Preeti Kabra

Department of Electrical Engineering, Koneru Lakshmaiah Education Foundation

Vijaywada, India

Email: mail.preeti.kabra@gmail.com

## 1. INTRODUCTION

In modern power systems, it is a mandate of utilizing real-time measurements for better control and management of the system. The real-time measurements [1] help us to even protect the devices connected to the system during fault conditions. With faster measurement readings taken from the system, a rapid response can be created avoiding many fatal conditions. This can be achieved using phasor measuring units (PMU) devices [2] connected at different locations of the power system. The placement of these devices can also be selected as per the requirement of sensitive devices. PMUs are used for multiple applications including assessment of power system stability and security and improving grid protection. These PMUs telecommunication devices have an issue of interfacing with external signals introducing disturbance and creating errors in the measured signals. These measured signals also have disruptions when the grid system is induced by any fault on the transmission lines [3].

For the analysis of different data measured by the PMU measuring devices an IEEE 14 bus system is considered with fault introduced at different locations of the bus system [4]. The signals from the PMU devices are compared with nominal operating conditions with bad data created when a fault is introduced in the bus system. Figure 1 shows IEEE 14 bus system, a single-line diagram with multiple sources and loads connected at different locations.

As observed the bus system [4] comprises different modules connected to different buses. Most of the buses have loads that are fed through three generators. Two synchronous condensers are also integrated into the system for injection of reactive power improving the voltage profile of the buses. These synchronous condensers can be replaced with static condensers which are capacitive VAR devices compensating reactive power [5]. The data for the modeling of 14 bus system is as shown in Table 1 to Table 4 as transmission line data, static condenser data. Load data and generator rating respectively below.

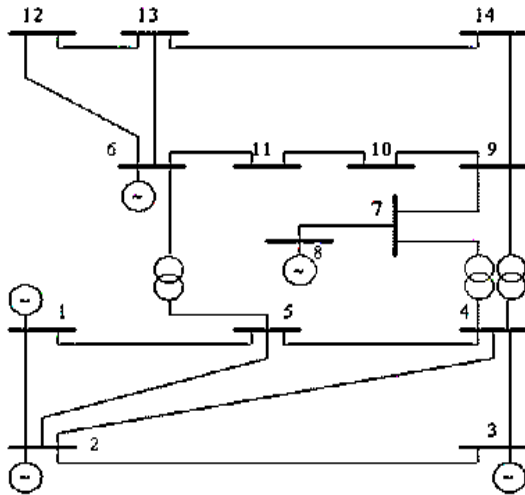


Figure 1. Single line diagram of IEEE 14 bus system

Table 1. Transmission line data

Line no.	From bus	To bus	Line resistance	Line reactance
1	1	2	0.01958	0.05927
2	1	5	0.05513	0.23204
3	2	3	0.05899	0.18797
4	2	4	0.06322	0.18632
5	2	5	0.05595	0.18388
6	3	4	0.05301	0.18103
7	4	5	0.02435	0.03511
8	4	7	0	0.15071
9	4	9	0	0.66718
10	5	6	0	0.27802
11	6	11	0.08498	0.1789
12	6	12	0.14491	0.28881
13	6	13	0.08015	0.24227
14	7	8	0	0.17515
15	7	9	0	0.12521
16	9	10	0.02191	0.0825
17	9	14	0.15761	0.32148
18	10	11	0.08325	0.18297
19	12	13	0.22072	0.18828
20	13	14	0.17063	0.35262

Table 2. Static condenser data

Condenser bus no.	Qmax (MVAR)
3	40 MVAR
9	19 MVAR

Table 3. Load data

Bus no.	P (MW)	Q (MVAR)	Bus no.	P (MW)	Q (MVAR)
1	0	0	8	0	0
2	21.7	12.7	9	29.5	16.6
3	94.2	19	10	9	5.8
4	47.8	-3.9	11	3.5	1.8
5	7.6	1.6	12	6.1	1.6
6	11.2	7.5	13	13.5	5.8
7	0	0	14	14.9	5

Table 4. Generators ratings

Generator no.	P min	P max
1	10.5 MW	165 MW
2	19.8 MW	82 MW
3	21 MW	45 MW

The modeling of the bus system is carried out using the above data with given parameters of generators, transmission lines, static condenser, and load data. The total system has an apparent power base value (Sbase) of 100 MVA and the voltage of the distribution system is considered to be 11 kV. Therefore, the base voltage (Vbase) value is 11 kV which makes the base impedance (Zbase) value given as:

$$\begin{aligned}
 Z_{base} &= \frac{kV_{base}^2}{MVA_{base}} \\
 &= \frac{11^2}{100} = 1.21 \text{ ohms}
 \end{aligned}
 \tag{1}$$

with the above impedance value, the transmission lines resistance and inductances are calculated. The inductance of the line for the given reactance ( $X$ ) is given as:

$$L_{line} = \frac{X_{line}}{\omega} \quad (2)$$

here,  $\omega$  is the angular frequency of the grid system taken as  $2\pi \cdot 50 = 314.15$  rad/sec.

The above IEEE 14 bus system is integrated with PMU [6] at all the given buses with three-phase voltages and currents measurements taken. The system is later included with a fault at one of the transmission lines and later updated with unified power quality conditioner (UPQC) module [7] connected at weakest bus 14. In this paper, section 1 is included with an introduction to the considered test system and modules followed by PMU devices modeling in section 2. In further section 3, the UPQC module configuration is discussed. In section 4 the simulation results and analysis are carried out with a comparison of nominal operating condition data, bad data during a fault, and updated data with the UPQC module is compared. The final section 5 is included with the conclusion to this paper with results discussion followed by references used in this paper.

## 2. PMU MODULE

A phasor measuring unit (PMU) is used to monitor transmission line data in real-time mode with time synchronization for widely located different substations. It gives magnitude as well as phase angle which makes it more advantageous over SCADA [8]. All the measurements in an electrical system vary as per the changes taking place in the grid modules. All these measurements are set with benchmark-defined values during normal and stable operating conditions. Any data that deviates from the path of these benchmark set values [9] during different operating conditions is considered bad data. As mentioned previously bad data can be created when the system is introduced with any fault or any external factor interference. These faults can be either on the transmission lines or at generators or even on the load side of the grid system [10]. The dynamic properties of each bus are noted and can be used for the analysis of the system during these faults which can be used for protection and security in the future.

The main feature of PMU is principal component analysis (PCA) which determines different components of the signal. These components can be compared to get bad data generated in the signal during disturbances. PCA helps to get lower dimension data which comprises maximum data variables increasing the resolution of the data needed [11], [12]. Different measurements can be taken from the PMU module comprising voltage magnitudes, current magnitudes, frequencies, or powers. In further detailing of these parameters multiple measurements like positive sequence component, negative sequence component, and zero sequence components can also be achieved [13], [14].

Different measurements have their calculation components which generate data for comparison. In MATLAB Simulink software multiple blocks are used to record the data achieved while operating the IEEE 14 bus system. The main block for measuring the magnitudes of bus voltages and currents is the 'sequence analyzer' taken from the 'power system' toolbox. The parameters of the 'sequence analyzer' are shown in Figure 2.

As seen the fundamental frequency of the IEEE 14 bus system is considered as 50 Hz and we are analyzing the fundamental harmonic component which is  $n=1$ . All three components positive, negative and zero can be analyzed at specific sampling time  $T_s$ . The lower the sampling time  $T_s$  the higher the data points [15] achieved which helps to store more data for analysis [16]. In the 'sequence analyzer' block even the angle of the voltages and currents can be determined. Along with this block for measuring the fundamental frequency of the buses a phase locked loop (PLL) block is taken from the 'power systems' toolbox. The parameters of the PLL block are shown in Figure 3.

As observed the minimum frequency limit is set at 45 Hz for the grid system with a fundamental frequency of 50 Hz. The PID regulator gains are set as per the required response of the block. For faster response, the rate of change of frequency needs to be increased. The cutoff frequency value mitigates the disturbances in the measured data. The recorded data of voltage magnitudes, current magnitudes, fundamental frequency, and voltage phase angles of an IEEE 14 bus system when operating in normal conditions are shown in the graphs.

- During normal operating condition: Figure 4 to Figure 7 shows voltage magnitude, current magnitude, frequency, and phase angle of all 14 buses respectively during the normal operating condition. All these graphs are taken with a simulation time of 1sec and the stabilized values are displayed on the right of the graph. The IEEE 14 bus system is induced with a fault at one of the transmission lines and the data is recorded. A fault is introduced between bus 4 and 5 with a 3-phase to ground symmetrical fault for

two cycles from 0.5 to 0.52sec of simulation time. Below are the graphical bad data achieved during this condition.

During fault condition: Figure 8 to Figure 11 shows voltage magnitude, current magnitude, frequency, and phase angle of all 14 buses respectively during a fault condition. As seen in the time domain graphs, bad data is created during the time 0.5 to 0.55sec due to a fault on the transmission line. For improvement in the operating conditions during a fault, an external device is connected to the weakest bus. The system is further updated with UPQC and the data is compared with normal, bad, and improvised conditions.

Sequence Analyzer (mask) (link)  
 Compute the positive-, negative-, and zero-sequence components of a three-phase signal.

Parameters

Fundamental frequency (Hz):  
 50

Harmonic n (1=fundamental):  
 1

Sequence: Positive Negative Zero

Initial input [ Mag, Phase (degrees) ]:  
 [1, 0]

Sample time:  
 Ts

Figure 2. Sequence analyzer parameters

Parameters

Minimum frequency (Hz):  
 45

Initial inputs [ Phase (degrees), Frequency (Hz) ]:  
 [0, 50]

Regulator gains [ Kp, Ki, Kd ]:  
 [180, 3200, 1]

Time constant for derivative action (s):  
 1e-4

Maximum rate of change of frequency (Hz/s):  
 12

Filter cut-off frequency for frequency measurement (Hz):  
 25

Sample time:  
 Ts

Enable automatic gain control

Figure 3. PLL block parameters

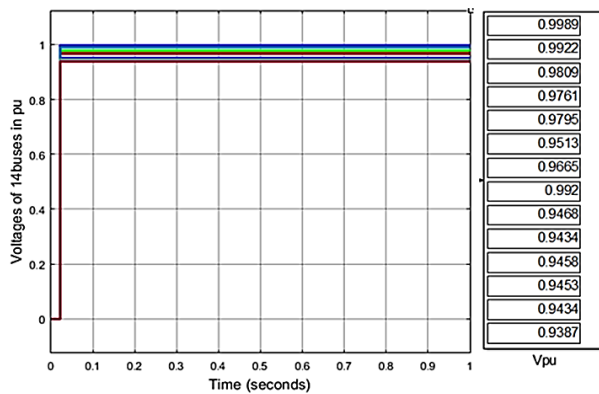


Figure 4. Voltage magnitudes of all 14 buses

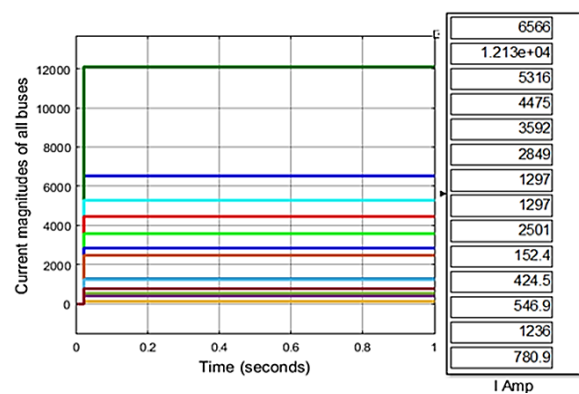


Figure 5. Current magnitudes of all 14 buses

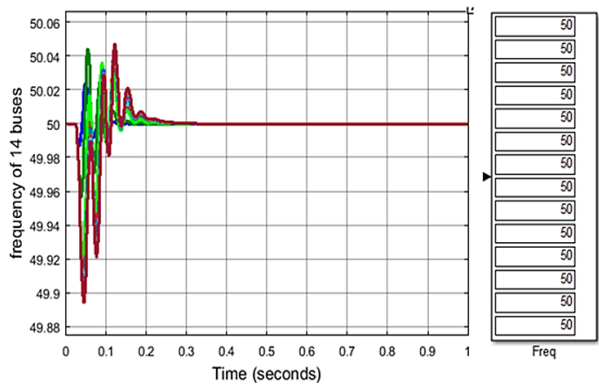


Figure 6. Frequency of all 14 buses

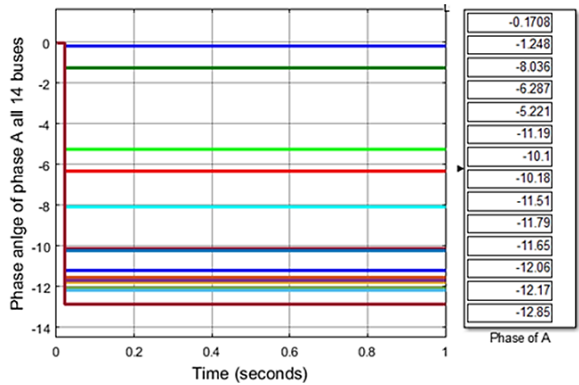


Figure 7. Phase angle of all 14 buses

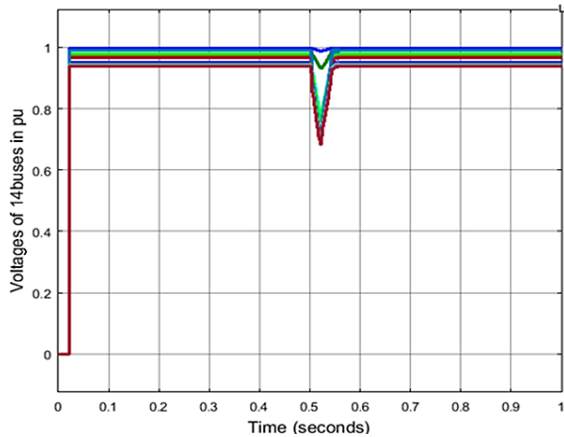


Figure 8. Voltage magnitudes of all 14 buses

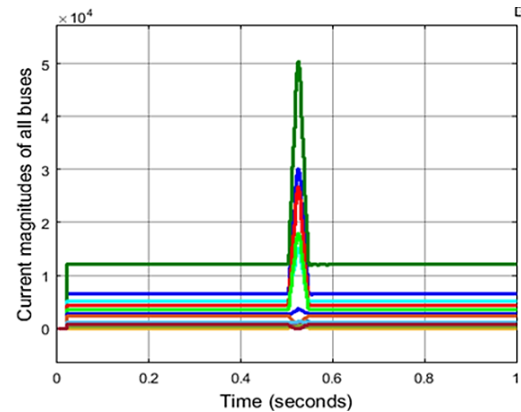


Figure 9. Current magnitudes of all 14 buses

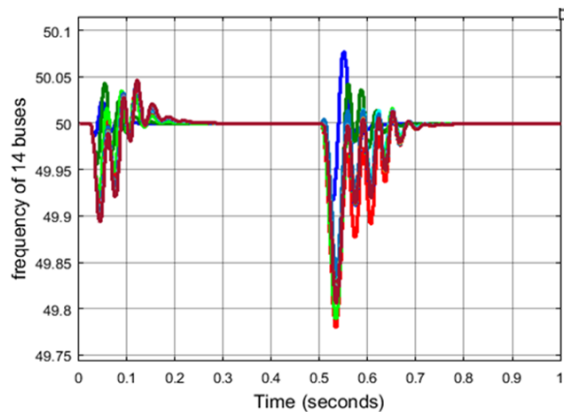


Figure 10. Frequency of all 14 buses

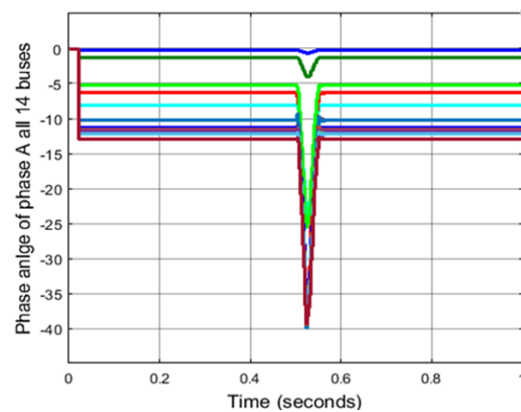


Figure 11. Phase angle of all 14 buses

### 3. UPQC CONFIGURATION

UPQC [17] is a traditional device with two modules connected to the grid in series and parallel connections. The series module is considered a dynamic voltage restorer (DVR) [18] and the shunt module is considered a synchronous static compensator (STATCOM). Each module comprises one voltage source converter (VSC) which converts AC-DC and DC-AC as per the requirement [19]. Both the VSCs are connected to the grid through inductive filters for harmonics reduction. Each VSC comprises 6-IGBT switches modeled in 3-legged format for connection to 3-ph lines. The VSC has two sides, a 3-ph AC side, and a DC side. The 3-ph AC side is connected to the grid and the DC side is connected to a common DC link capacitance for energy storage. The DC link capacitance is a support element for the VSC which helps to mitigate different issues in the grid. The DVR module (series) compensates for voltage fluctuations and the STATCOM module (shunt) compensates for harmonics [20]. The internal modeling of the UPQC device can be seen in Figure 12.

The 6-switches in each module need to be controlled for the compensation of voltages and harmonics in the grid. Both the VSC modules are controlled with synchronized pulse generation concerning the source voltages. The DVR controller [21] generates references as voltage components and the STATCOM controller generates references as current components. Figure 13 is the controller for the DVR module with the Sin PWM technique [22].

As observed in Figure 13 the controller takes the input of source voltages ( $V_{Sabc}$ ) and load voltages ( $V_{Labc}$ ) for the generation of series reference voltage components ( $V_{SEabc}^*$ ). To generate these components both  $V_{Sabc}$  and  $V_{Labc}$  signals are converted to dq-components [23] and compared to generate the error voltages. The Park's transformation is given as:

$$\begin{bmatrix} V_d \\ V_q \\ V_0 \end{bmatrix} = \begin{bmatrix} \sin \theta & -\cos \theta & 0 \\ \cos \theta & \sin \theta & 0 \\ 0 & 0 & 1 \end{bmatrix} \begin{bmatrix} V_a \\ V_b \\ V_c \end{bmatrix} \tag{3}$$

the series reference dq-components (VSEdq) are given as:

$$V_{SEd}^* = (K_P + \int K_I) (V_{Ld}^* - V_{sd}) - (V_{Ld} - V_{sd}) \tag{4}$$

$$V_{SEq}^* = (K_P + \int K_I) (V_{Lq}^* - V_{sq}) - (V_{Lq} - V_{sq}) \tag{5}$$

here,  $K_p$  and  $K_i$  are the gain of the PI controller which are set by tuning the module until stabilized voltages are achieved. The series reference dq-components are converted to abc components using inverse Park's transformation for Sin PWM technique pulse generation.

$$\begin{bmatrix} V_a \\ V_b \\ V_c \end{bmatrix} = \begin{bmatrix} \sin \theta & \cos \theta & 1 \\ \sin(\theta - \frac{2\pi}{3}) & \cos(\theta - \frac{2\pi}{3}) & 1 \\ \sin(\theta + \frac{2\pi}{3}) & \cos(\theta + \frac{2\pi}{3}) & 1 \end{bmatrix} \begin{bmatrix} V_d \\ V_q \\ V_0 \end{bmatrix} \tag{6}$$

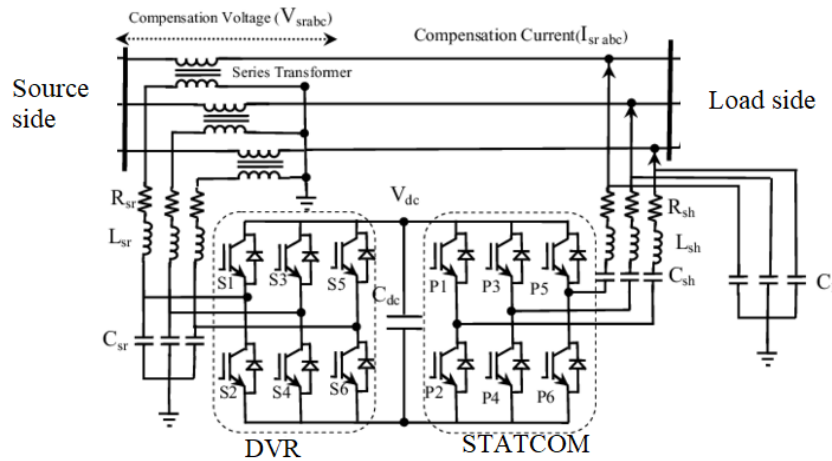


Figure 12. UPQC internal modeling

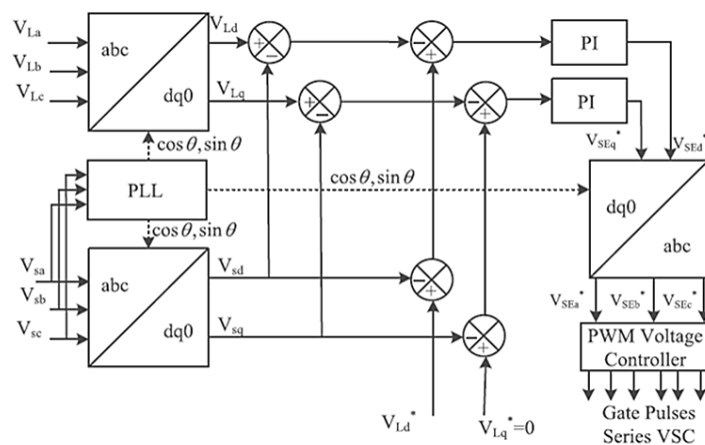


Figure 13. DVR module control structure

Similar to this the STATCOM module also has many components taken as input for generation reference current components. The controller of the STATCOM [24] is updated with the virtual inertia concept which makes this static device operate as a dynamic synchronous condenser for better results generation. The updated virtual inertia controller of the STATCOM can be seen in Figure 14.

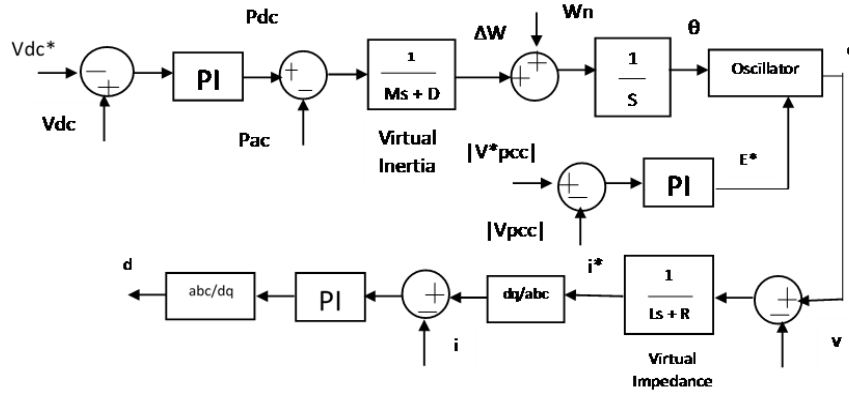


Figure 14. Virtual impedance integrated STATCOM controller

In Figure 14, controller  $V_{dc}^*$  is the reference [25] DC link voltage and  $V_{dc}$  is the measured DC link voltage. The  $P_{dc}$  reference is given as:

$$P_{dc} = (K_P + \int K_I) (V_{dc}^* - V_{dc}) \tag{7}$$

The change in angular frequency is generated concerning  $P_{dc}$  and  $P_{ac}$  values.

$$\Delta\omega = \left(\frac{1}{M_s + D}\right) (P_{dc} - P_{ac}) \tag{8}$$

The reference phase angle for the generation of reference voltage signals is given as:

$$\theta = \int (\omega_n + \Delta\omega_n) \tag{9}$$

The magnitude for the reference voltage signals is taken as:

$$E^* = (K_p + \int K_i) * (|V_{pcc}^*| - |V_{pcc}|) \tag{10}$$

Therefore, the reference current  $i^*$  components is given as (11).

$$i^* = \left(\frac{1}{L_s + R}\right) (e - v) \tag{11}$$

In the above equation  $e = E^* \sin\theta$ . L and R are the inductance and resistance of the series inductor connected to the shunt VSC [23]. The reference current ( $i^*$ ) is converted to dq-components which are compared to measured current  $i_{dq}$ -components of the VSC output.

The final reference voltage dq-component is given as (12).

$$V_{dq}^* = (K_P + \int K_I) (i_{dq}^* - i_{dq}) \tag{12}$$

This final reference voltage dq-component is converted to abc using (6) and the final reference voltage signals are fed to Sin PWM technique for controlling the shunt VSC. The IEEE 14 bus system is updated with UPQC connected at the weakest bus (bus no. 14) and the results are compared with normal data, bad data during fault, and improvised data with UPQC.

#### 4. SIMULATION RESULTS

The modeling of the IEEE 14 bus system with UPQC module connected at bus 14 and fault between bus 4 and 5 is done with MATLAB Simulink software. The model is run for 1 sec with fault set from 0.5 to 0.52 sec in all three models. Figure 15 shows voltage and current magnitudes of all 14 buses during fault condition with UPQC and Figure 16 shows frequencies and Phase angles of phase A of all the 14 buses during fault conditions with UPQC. Figure 17 shows the comparison of the voltage magnitudes and frequency respectively when the data is recorded in normal (blue), fault (red), and integrated with UPQC (green) operating conditions for bus 14. It indicates bad data which appeared in normal conditions can be improvised with virtual synchronous machine (VSM)-UPQC and ultimately improve the quality of data.

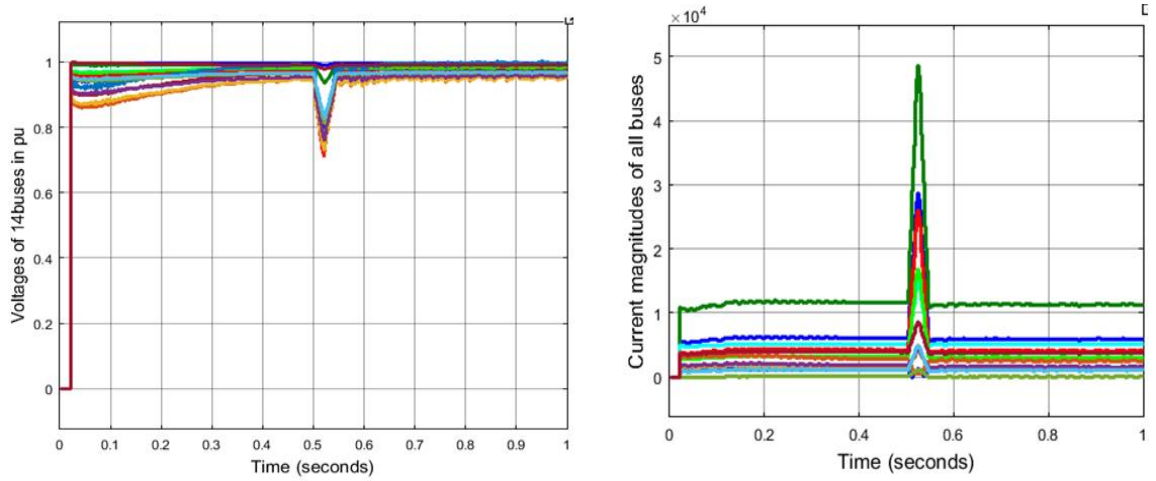


Figure 15. Voltages and currents magnitudes of all 14 buses during fault condition with UPQC

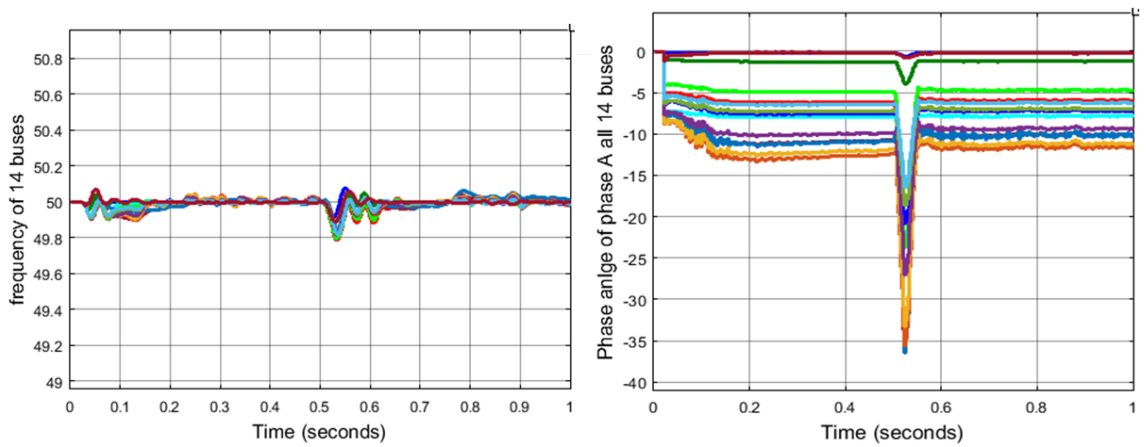


Figure 16. Frequencies and phase angles of phase A of all the 14 buses during fault conditions with UPQC

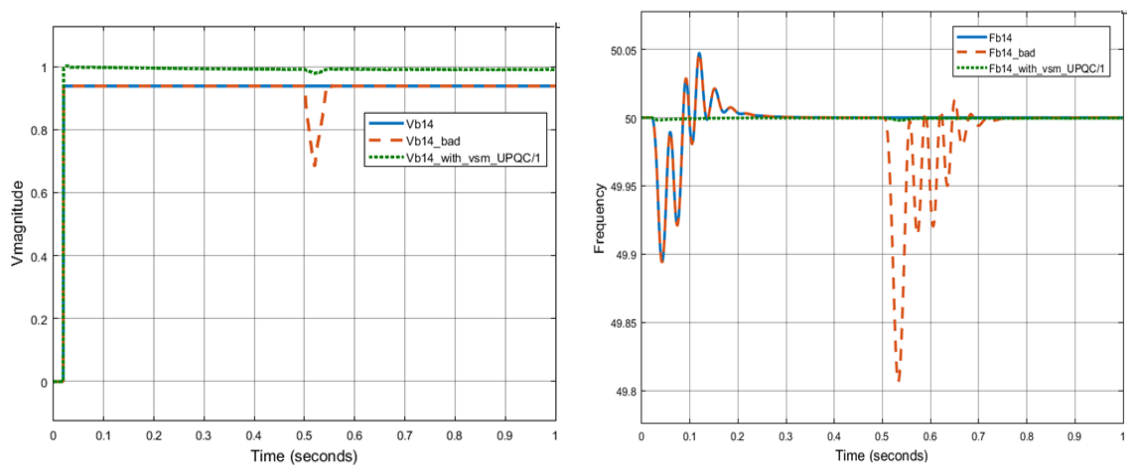


Figure 17. Voltage magnitude and frequency comparison of bus 14

### 5. CONCLUSION

Successful implementation of the IEEE 14 bus system as per the data and integration of the UPQC module into the grid system is done. The bus system is introduced with a fault on one of the transmission line



creating bad data in the measurements. The bad data is compared to normal data which is achieved during the normal operating condition. Four parameters are considered for data recording which include voltage magnitudes, current magnitudes, frequencies, and phase angles. All the data generated by the PMU are plotted in graphical format for comparison to determine the difference between good and bad data. With further updating the bus system with UPQC the new improvised data is also compared showing the improvement in voltage magnitude and frequency of the buses. For our analysis, the UPQC device is connected to the weakest bus (bus no. 14) and the data achieved is compared. Concluding that the bad data created due to fault in the system is stabilized by the UPQC device with lower voltage magnitude drop and lower frequency disturbance. The voltage magnitude is maintained near unity and the frequency is remaining at 50 Hz even during the fault condition.




## REFERENCES

- [1] P. Kabra and S. R. Donepudi, "Power quality improvement and analysis of interconnected bus system with PMU using VSM-STATCOM," *International Journal of Applied Power Engineering (IJAPE)*, vol. 11, no. 1, pp. 52-61, Mar. 2022, doi: 10.11591/ijape.v11.i1.pp52-61.
- [2] C. Lin, W. Wu, and Y. Guo, "Decentralized robust state estimation of active distribution grids incorporating microgrids based on PMU measurements," in *IEEE Transactions on Smart Grid*, vol. 11, no. 1, pp. 810-820, Jan. 2020, doi: 10.1109/TSG.2019.2937162.
- [3] Y. Zhang, Y. Xu, and Z. Y. Dong, "Robust ensemble data analytics for incomplete PMU measurements-based power system stability assessment," in *IEEE Transactions on Power Systems*, vol. 33, no. 1, pp. 1124-1126, Jan. 2018, doi: 10.1109/TPWRS.2017.2698239.
- [4] J. Zhao, G. Zhang, M. L. Scala, and Z. Wang, "Enhanced robustness of state estimator to bad data processing through multi-innovation analysis," in *IEEE Transactions on Industrial Informatics*, vol. 13, no. 4, pp. 1610-1619, Aug. 2017, doi: 10.1109/TII.2016.2626782.
- [5] N. A. Daw and A. H. Salih, "Choosing the best place of static VAR compensator in IEEE 14 bus system to improve voltage using Neplan software," *2019 19th International Conference on Sciences and Techniques of Automatic Control and Computer Engineering (STA)*, 2019, pp. 30-35, doi: 10.1109/STA.2019.8717247.
- [6] Y. Lin and A. Abur, "A highly efficient bad data identification approach for very large scale power systems," in *IEEE Transactions on Power Systems*, vol. 33, no. 6, pp. 5979-5989, Nov. 2018, doi: 10.1109/TPWRS.2018.2826980.
- [7] X. Wang *et al.*, "Online calibration of phasor measurement unit using density-based spatial clustering," in *IEEE Transactions on Power Delivery*, vol. 33, no. 3, pp. 1081-1090, Jun. 2018, doi: 10.1109/TPWRD.2017.2688356.
- [8] W. Ur Rahman, M. Ali, C. A. Mehmood, and A. Khan, "Design and implementation for wide area power system monitoring and protection using phasor measuring units," *WSEAS Transactions on Power systems*, vol. 8, no. 2, pp. 57-64, 2016.
- [9] K. Mahapatra, N. R. Chaudhuri, and R. Kavasseri, "Online bad data outlier detection in PMU measurements using PCA feature-driven ANN classifier," *2017 IEEE Power & Energy Society General Meeting*, 2017, pp. 1-5, doi: 10.1109/PESGM.2017.8273997.
- [10] B. Gou and R. G. Kavasseri, "Unified PMU placement for observability and bad data detection in state estimation," *IEEE Transactions on Power Systems*, vol. 29, no. 6, pp. 2573-2580, Nov. 2014, doi: 10.1109/TPWRS.2014.2307577.
- [11] A. Tarali and A. Abur, "Bad data detection in two-stage state estimation using phasor measurements," *2012 3rd IEEE PES Innovative Smart Grid Technologies Europe (ISGT Europe)*, 2012, pp. 1-8, doi: 10.1109/ISGTEurope.2012.6465712.
- [12] M. B. Do Couto Filho, J. C. Stacchini de Souza, and R. Guimaraens, "Enhanced bad data processing by phasor-aided state estimation," in *IEEE Transactions on Power Systems*, vol. 29, no. 5, pp. 2200-2209, 2014, doi: 10.1109/TPWRS.2014.2304620.
- [13] A. S. Costa, A. Albuquerque, and D. Bez, "An estimation fusion method for including phasor measurements into power system real-time modeling," in *IEEE Transactions on Power Systems*, vol. 28, no. 2, pp. 1910-1920, May 2013, doi: 10.1109/TPWRS.2012.2232315.
- [14] O. Vuković and G. Dán, "Security of fully distributed power system state estimation: detection and mitigation of data integrity attacks," in *IEEE Journal on Selected Areas in Communications*, vol. 32, no. 7, pp. 1500-1508, Jul. 2014, doi: 10.1109/JSAC.2014.2332106.
- [15] A. Tajer, "Energy grid state estimation under random and structured bad data," in *2014 IEEE 8th Sensor Array and Multichannel Signal Processing Workshop (SAM)*, 2014, pp. 65-68, doi: 10.1109/SAM.2014.6882339.
- [16] K. Mahapatra, N. R. Chaudhuri, and R. Kavasseri, "Bad data detection in PMU measurements using principal component analysis," *2016 North American Power Symposium (NAPS)*, 2016, pp. 1-6, doi: 10.1109/NAPS.2016.7747928.
- [17] K. Saicharan and A. R. Gupta, "Effective placement of UPQC and DG in radial distribution system," *2020 First IEEE International Conference on Measurement, Instrumentation, Control and Automation (ICMICA)*, 2020, pp. 1-6, doi: 10.1109/ICMICA48462.2020.9242721.
- [18] S. Tiwari, R. Agrawal, D. Agrawal, and D. Verma, "Performance analysis of DVR and UPQC to improve power quality of three-phase distribution system," *2021 IEEE 2nd International Conference On Electrical Power and Energy Systems (ICEPES)*, 2021, pp. 1-5, doi: 10.1109/ICEPES52894.2021.9699503.
- [19] A. Srivastav, A. Chauhan, and A. Tripathi, "Mitigation of harmonics in voltage and current using UPQC," *International Conference on Power Electronics & IoT Applications in Renewable Energy and its Control (PARC)*, 2020, pp. 456-460, doi: 10.1109/PARC49193.2020.236654.
- [20] C. Li, R. Burgos, I. Cvetkovic, D. Boroyevich, L. Mili, and P. Rodriguez, "Analysis and design of virtual synchronous machine based STATCOM controller," *2014 IEEE 15th Workshop on Control and Modeling for Power Electronics (COMPEL)*, 2014, pp. 1-6, doi: 10.1109/COMPEL.2014.6877134.
- [21] J. Yu, Y. Xu, Y. Li, and Q. Liu, "An inductive hybrid UPQC for power quality management in premium-power-supply-required applications," in *IEEE Access*, vol. 8, pp. 113342-113354, 2020, doi: 10.1109/ACCESS.2020.2999355.
- [22] A. M. Rauf and V. Khadkikar, "An enhanced voltage sag compensation scheme for dynamic voltage restorer," in *IEEE Transactions on Industrial Electronics*, vol. 62, no. 5, pp. 2683-2692, May 2015, doi: 10.1109/TIE.2014.2362096.




- [23] S. Golestan, M. Ramezani, J. M. Guerrero, and M. Monfared, "dq-frame cascaded delayed signal cancellation- based PLL: analysis, design, and comparison with moving average filter-based PLL," in *IEEE Transactions on Power Electronics*, vol. 30, no. 3, pp. 1618-1632, Mar. 2015, doi: 10.1109/TPEL.2014.2315872.
- [24] Q. -C. Zhong, P. -L. Nguyen, Z. Ma, and W. Sheng, "Self-synchronized synchronverters: inverters without a dedicated synchronization unit," in *IEEE Transactions on Power Electronics*, vol. 29, no. 2, pp. 617-630, Feb. 2014, doi: 10.1109/TPEL.2013.2258684.
- [25] A. Rodríguez-Cabero, J. Roldán-Pérez, and M. Prodanovic, "Virtual impedance design considerations for virtual synchronous machines in weak grids," *IEEE Journal of Emerging and Selected Topics in Power Electronics*, vol. 8, no. 2, pp. 1477-1489, Jun. 2020, doi: 10.1109/JESTPE.2019.2912071.

## BIOGRAPHIES OF AUTHORS






**Preeti Kabra**    received B.E. degree in Electrical, Electronics and Power from Government college of Engineering, Aurangabad (MH) in 2000 and MTech degree from Jawaharlal Nehru Technical University, Hyderabad (TS). Currently working as Assistant Professor in Deccan College of Engineering and Technology, Hyderabad and Research scholar of KLEF, Vijaywada (AP). Her main area of interest is power system automation, smart grid, WAMS, and synchro phasor technology. She can be contacted at email: mail.preeti.kabra@gmail.com.



**Suraparaju Venkata Naga Lakshmi Lalitha**    is working as a Professor in the Department of Electrical and Electronics Engineering, Koneru Lakshmaiah Education Foundation (K.L.E.F.) deemed to be University, Vijayawada, India. She obtained her Master of Technology and Ph.D. degree from National Institute of Technology, Warangal, Telangana, India. She obtained her B. Tech degree from Sri Venkateshwara University, Tirupathi, A.P., India. Her areas of research include power system restructuring, distribution systems, smart grids, meta heuristic techniques application to power system, Wide area power system monitoring and protection in dynamic state using synchronized phasor measurements, static and dynamic state estimation incorporating synchro phasor measurements, transient fault detection and analysis of microgrid connected power system. She can be contacted at email: lalitha@kluniversity.in.



**Sudha Rani Donepudi**    received B. Tech degree in Electrical and Electronics Engineering from JNTU Hyderabad in 2006, M.E. degree from Andhra University in 2008, Visakhapatnam, and Doctoral degree from National Institute of Technology Warangal in 2016. Currently working as Professor in Sri Vasavi Engineering College, West Godavari, Andhra Pradesh. Her areas of interest are power system automation, smart grid, application of optimization in power systems, and electrical vehicles. She can be contacted at email: sudha179@nitw.ac.in.